ARTICLE

OBC
www.rsc.org/obc

Is the ring conformation the most critical parameter in lipase-catalysed acylation of cycloalkanols?†

Laura M. Levy, Iván Lavandera and Vicente Gotor*
Departamento de Química Orgánica e Inorgánica, Facultad de Química, Universidad de Oviedo, 33006 Oviedo, Spain. E-mail: vgs@fq.uniovi.es; Fax: +34-985103448; Tel: +34-985103448

Received 11th June 2004, Accepted 27th July 2004
First published as an Advance Article on the web 23rd August 2004

CAL-B catalysed the resolution of several five and six-membered cyclic β-hydroxy esters efficiently with the exception of the *cis*-cyclohexanol (±)-**4**. When employing molecular modelling techniques the conformation turned out to be the most important determinant for their reactivity towards *O*-acetylation. In all cases, the *R* enantiomers reacted faster than the *S* enantiomers since the reactive intermediates of the former can adopt more favourable ring conformations and thus experience less steric hindrance in the active site. Furthermore, the minimised structure for the main conformer of *R*-**4** showed that the axial hydrogens in the 3 and 5-positions with respect to the hydroxyl group prevent the enzymatic reaction.

1. Introduction

The kinetic resolution of racemic mixtures with lipases is an attractive means for the preparation of enantiomerically pure molecules[1] and is used as a major method for their industrial scale production.[2]

Several 5 and 6-membered cyclic alcohols have been resolved by lipase-catalysed acylation reactions.[3,4] Amongst them, different 1,2-disubstituted cycloalkanols, which are important chiral building blocks for the asymmetric synthesis of biologically active compounds, have been obtained enantiomerically pure using this tool.[5,6] These resolutions show some common trends, such as, first, the *R* enantiomer is always preferred by the lipase, secondly, cyclopentanols react more rapidly than cyclohexanols, and thirdly, the *cis* isomers react more slowly than their *trans* analogues. During the development of the resolution of several five, six and seven-membered cyclic *cis* and *trans*-β-hydroxy esters (Fig. 1) with lipases A and B from *Candida antarctica* (CAL-A and CAL-B), we noticed that CAL-B reacted very efficiently with all *R* enantiomers except in the case of the *cis*-cyclohexanol.[7] There are other examples known in the literature in which the *cis*-2-substituted cyclohexanols do not react with lipases, even when the corresponding *cis*-2-substituted cyclopentanols do.[3b,8] However, in some cases it has been shown that the *cis*-2-substituted cycloheptanol derivatives react under the same conditions.[7,9]

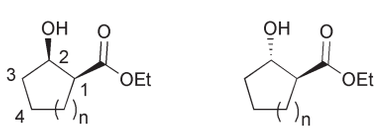

n= 1, 2, 3

Fig. 1

Conformational effects could account for this tendency, since in general hydroxyl groups react more slowly in axial than in equatorial position in lipase-catalysed resolutions.[3b,10] The same is true for non-biocatalysed transformations. For example, Eliel and Biros showed that the acylation of 2-alkylcyclohexanols occurs faster with the *trans* isomers (OH equatorial) than with the *cis* isomers (OH axial) due to steric and polar effects.[11] Pasto and Rao also recorded a similar trend in 2,5-di-*tert*-butylcyclohexanol derivatives.[12]

Computer-aided molecular modelling is a potent tool to explain many experimental results in biotransformations.[13] The force field methods relate the geometry with the potential energy of a molecule using an analytical function. Amongst them, AMBER force field is one of the most commonly used for protein structures.[14] Conformations can be either randomly or manually generated by rotation of the dihedral angles within the molecule. Crystal structures of the enzyme can be studied with its ligand bound, and both the electrostatic and steric interactions are considered. Thus, modelling of these transition states helps to understand the mechanism,[15] and the selectivity[16] of the enzymes.

In this work, we have modelled the intermediates in the CAL-B-catalysed acetylation of five and six-membered cyclic *cis* and *trans*-β-hydroxy esters (Fig. 1, n = 1, 2), in order to explain the excellent selectivity seen with the *R*-enantiomers. Together with NMR spectroscopy, the lack of reactivity of the *cis*-cyclohexanol derivative compared to the five-membered analogue was also studied.

2. Results and discussion

2.1. Resolution of cyclic β-hydroxy esters by lipase-catalysed acetylation

As mentioned in the introduction, we have developed the resolution of several five, six, and seven-membered cyclic β-hydroxy esters *via* CAL-B-catalysed acetylation with vinyl acetate in *tert*-butyl methyl ether at 30 °C (Scheme 1).[7] Under these reaction conditions (Table 1), the acylation of the *trans* isomers (±)-**1** and (±)-**2** took place smoothly, yielding both the *S*-substrates and the *R* products enantiomerically pure. When the same methodology was applied to the *cis*-configured β-hydroxy esters, the *R* enantiomer of the five-membered derivative (±)-**3** was rapidly acetylated. However, CAL-B showed very low activity towards *cis*-cyclohexanol (±)-**4**, obtaining only 5% conversion after 2 days, despite exhibiting again complete enantiodiscrimination (E > 200).

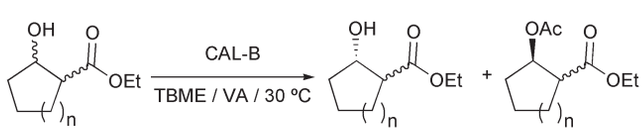

Scheme 1

2.2. Molecular modelling

Starting with the X-ray crystal structure of CAL-B (1LBS),[18] we modelled the analogues of the second tetrahedral intermediate

† Electronic supplementary information (ESI) available: complete ^{1}H-NMR spectral data are shown. Furthermore, some extensive modelling figures are included. See http://www.rsc.org/suppdata/ob/b4/b408861a/

DOI: 10.1039/b408861a

Table 1 Resolution of cyclic β-hydroxy esters with CAL-B[a]

n[b]	Substrate	*t*/h	*c*[c]	*E*[c]
1 (*trans*)	(±)-**1**	1.3	50	>200
2 (*trans*)	(±)-**2**	1.7	50	>200
1 (*cis*)	(±)-**3**	2.7	50	>200
2 (*cis*)	(±)-**4**	48	5	>200

[a]See Ref. 7. [b]See Scheme 1. [c]Calculated from the e.e. of the substrate and the product. See Ref. 17.

in the acetylation of the cycloalkanols, since this transition state determines the rate and selectivity in a kinetic resolution of racemic alcohols (Fig. 2).

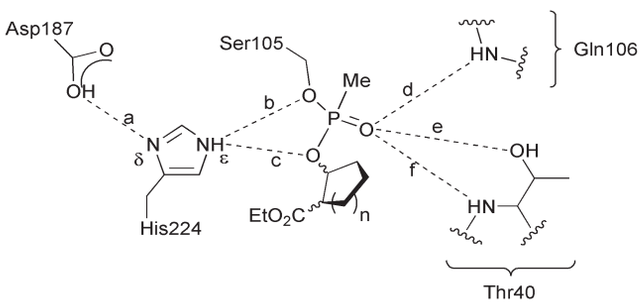

Fig. 2 Phosphonate intermediates used for molecular modelling in the acetylation of cyclopentanols (n = 1) or cyclohexanols (n = 2) catalysed by CAL-B. Key hydrogen bonds between the lipase and the intermediate are displayed as dashed lines (a–f).

In order to simplify the modelling process using molecular mechanics force fields, we chose the phosphonate analogues of these tetrahedral intermediates for minimisation calculations.[18] Geometry optimisation of the phosphonate containing a methoxy group attached to the phosphorus atom afforded a structure in which all key hydrogen bonds required for catalysis were present (Fig. 2).[19] Next, the whole molecule was added and minimised. Different conformations of these structures were systematically searched for and focused on those most likely to mimic catalytically productive transition states (see under Computational details). The following two criteria had to be fulfilled: the presence of all key hydrogen bonds within the active site and the lack of steric impediments between the phosphonate and the lipase.

The active site of CAL-B contains a large hydrophobic pocket (or acyl pocket) above the Asp-His-Ser catalytic triad and a medium-sized pocket (or nucleophile pocket) below it.[18] The acyl moiety of the intermediate lies in the large subsite (the methyl of the acetate in our case), while the carbocycle of the cycloalkanol binds to the medium-sized pocket. In general, the active site below the catalytic triad restricts the binding of the alcohol substrate to such an extent that only a few conformations were obtained with all the catalytic hydrogen bonds present.[19] Conformation and ring size proved to be most crucial when determining reactive intermediates.

2.2.1. Enzymatic acylation of *trans*-cyclohexanol (±)-2. First, we studied the CAL-B-catalysed acetylation of (±)-2. Cyclohexane derivatives are present in a two chair-equilibrium in solution, which lies on the side of the thermodynamically more stable one. *trans*-1,2-Disubstituted cyclohexanes virtually exist only in the conformation that places both substituents in equatorial positions.[20] Thus, only those structures with both the alcohol and the ester group placed in the less hindered positions were taken into account during the molecular modelling.

The best structure of the tetrahedral intermediate for the *O*-acetylation of *R*-**2** is shown in Fig. 3A. The cyclohexane ring fits perfectly into the medium-sized pocket with all key hydrogen bonds present (Row 1 in Table 2) and with no steric hindrance. Both substituents occupy equatorial positions and the ester

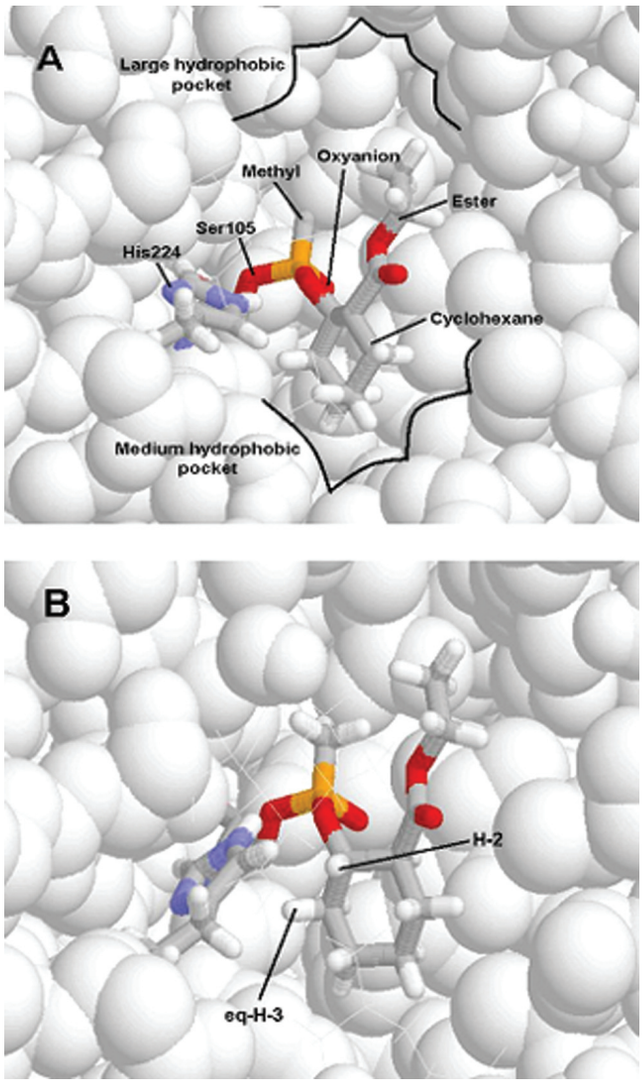

Fig. 3 Phosphonate models for the O-acetylation of cyclohexanol 2: A) R enantiomer; and B) S enantiomer. Red represents oxygen atoms, blue represents nitrogen atoms, and yellow represents phosphorus atoms. Above images display some amino acids in a wireframe representation to allow a better view of the structures.

moiety lies in the large pocket, with the oxygen of the carbonyl group pointing out towards the solvent.

In the case of the phosphonate analogue of *S*-**2**, the ring also binds to the medium-sized pocket (Fig. 3B). This time however, H-2 and eq-H-3, which are *trans* to the phosphonate group, are very close to the catalytic histidine despite rotation of both the cyclohexane moiety and the histidine group. As a consequence, three key hydrogen bonds are lost (Row 2 in Table 2).

The different orientations of the substrates in the active site, and the steric hindrance between the cyclohexane and His224 residue, appeared to be key determinants of the enzyme selectivity. This was also confirmed by the energies obtained for both structures, since the *R* intermediate was 4.2 kcal mol^{-1} more stable than the *S*-enantiomer.[21]

2.2.2. Enzymatic acylation of *trans*-cyclopentanol (±)-1. Next, we modelled the enzymatic acylation of *trans*-cyclopentanol (±)-**1**. Conformations of cyclopentanes have been much less studied. Nonetheless, it has been established that there are two symmetrical puckered conformations, the envelope (C_s) and the half-chair (C_2), with the energy barrier very low between both (Fig. 4). The most stable conformer of *trans*-cyclopentane-1,2-diol is shown in Fig. 4A (X = OH).[22] Normally, five-membered ring derivatives react enzymatically faster than cyclohexanes.[3] Accelerative factors could be, first, the smaller size of the cycle, which would produce less steric

Table 2 Key hydrogen bonds and energy in CAL-B-catalysed acetylation of cyclic *trans*- and *cis*-β-hydroxy esters of five and six members[a]

Row	Compound	Fig.[b]	H-bond distance/Å (angle)[c]						*E*/kcal mol^{-1}
			a	b	c	d	e	f	
1	(2*R*)-**2**	3A	3.02 (134°)	3.14 (131°)	2.91 (147°)	3.03 (160°)	2.75 (168°)	2.82 (170°)	0
2	(2*S*)-**2**	3B	**3.25 (124°)**	**3.31 (134°)**	2.91 (133°)	**3.39 (162°)**	2.76 (168°)	2.85 (168°)	+4.2[d]
3	(2*R*)-**4** (OH ax)	7A	3.06 (132°)	3.01 (146°)	**3.40 (139°)**	2.97 (161°)	2.78 (172°)	2.83 (166°)	+6.4[d]
4	(2*R*)-**4** (OH eq)	7B	3.07 (150°)	2.96 (128°)	2.95 (139°)	3.16 (155°)	2.80 (165°)	2.78 (166°)	+9.3[d]
5	(2*S*)-**4**	S4	**3.48 (126°)**	2.95 (127°)	**3.27 (113°)**	3.18 (160°)	2.72 (167°)	3.03 (165°)	+5.9[d]
6	(2*R*)-**1**	S1	3.03 (135°)	3.16 (129°)	2.83 (144°)	3.01 (157°)	2.77 (172°)	2.80 (172°)	0
7	(2*S*)-**1**	S2	**3.23 (127°)**	**3.32 (139°)**	2.85 (139°)	**3.55 (165°)**	2.76 (161°)	2.79 (159°)	+4.4[e]
8	(2*R*)-**3**	5	3.01 (134°)	2.91 (131°)	3.06 (149°)	2.85 (154°)	2.77 (174°)	2.85 (175°)	+2.4[e]
9	(2*S*)-**3**	S3	3.00 (133°)	3.15 (132°)	2.93 (155°)	3.09 (161°)	2.78 (168°)	3.16 (128°)	+4.1[e]

[a] Lost hydrogen bonds appear in bold. [b] See text. [c] Fig. 2 defines the hydrogen bonds. [d] Compared with the energy of Fig. 3A. [e] Compared with the energy of Fig. S1 (ESI).

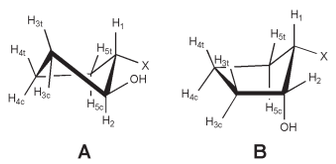

Fig. 4 Main conformation for: A) trans-1,2-disubstituted cyclopentanols; and B) cis-1,2-disubstituted cyclopentanols.

hindrance in the active site, and secondly, the greater ease of cyclopentanes to convert from one conformation into another, by this increasing the possibility of finding an acceptable disposition in the active site.

On the other hand, different conformations of cyclohexanes are more difficult to interconvert. Thus, if the lowest energy chair conformer does not fit into the active site in a successful orientation, it is less probable that the reaction takes place.

When computer modelling was used to minimise the intermediates of the *trans*-cyclopentane derivatives (±)-**1**, similar results to the six-membered analogues (±)-**2** were obtained. For *R*-**1**, the cycle fits into the medium subsite in a half-chair conformation without any steric impediments (Fig. 4A, X = CO_2Et), with all key hydrogen bonds present (Row 6 in Table 2). In contrast, for *S*-**1**, the ring lies in the medium-sized pocket in a less stable envelope conformer. Furthermore, H-2 and H-3c are too close to His224, destabilising the intermediate by 4.4 kcal mol^{-1} with respect to the *R* enantiomer (Row 7 in Table 2). Models are shown in electronic supplementary information (ESI)† as Fig. S1 and S2.

2.2.3. Enzymatic acylation of *cis*-cyclopentanol (±)-3. The most stable conformation of *cis*-cyclopentane-1,2-diol is a slightly distorted envelope, shown in Fig. 4B (X = OH).[22]

The phosphonate intermediate shown in Fig. 5 was chosen as the best model for the acetylation of *R*-**3**. As with the *trans* isomer, the ring binds perfectly to the medium-sized pocket, with the hydroxyl group in an axial position at the fold of the envelope and the ester located in a less hindered equatorial position at the flap of the envelope (Fig. 4B, X = CO_2Et). This group lies in the large hydrophobic subsite with the oxygen of the carbonyl pointing out towards the solvent. All key hydrogen bonds are present in this structure (Row 8 in Table 2). There are no significant steric interactions in the active site, only H-4c and H-5c being slightly closer to the catalytic histidine (Fig. 8A), but not enough to disrupt the interaction between this amino acid and the nucleophile. This may be the cause for the slower reaction with respect to the *trans* analogue, since the energy of the *cis* intermediate is 2.4 kcal mol^{-1} higher.

When the phosphonate analogue of *S*-**3** was modelled, a structure in which both groups occupied equatorial positions at the fold of the envelope was obtained, with a slightly higher energy (Fig. S3 in ESI†). Furthermore, the ester moiety lies too close to the His224 residue, moving away the cycle towards Thr40. As a result of this, a weaker interaction between this

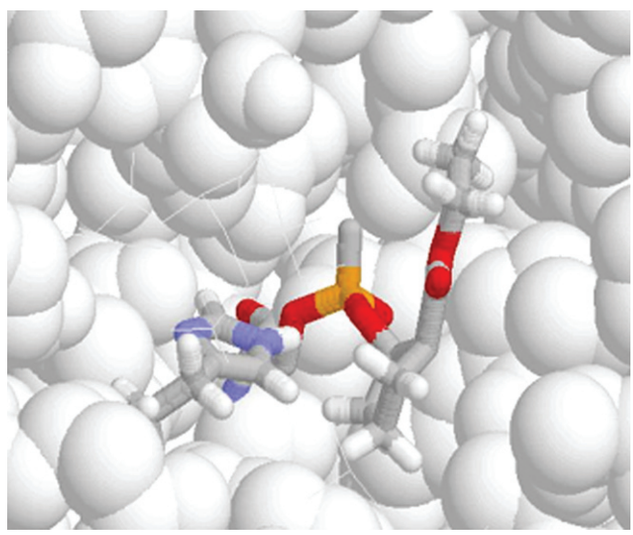

Fig. 5 Model for the *O*-acetylation of the *R* enantiomer of cyclopentanol **3**. The above image displays some amino acids in a wireframe representation to allow a better view of the structure.

amino acid and the oxyanion takes place (Row 9 in Table 2). This is also confirmed by the energies obtained for both structures, since the *R* intermediate is 1.7 kcal mol^{-1} more stable than the *S* analogue.

2.2.4. Enzymatic acylation of *cis*-cyclohexanol (±)-4. Next, we studied *cis*-cyclohexanol (±)-**4**. This substrate proved to be poor for CAL-B, observing almost no product formation even after 2 days. In this case, the ring conformation could be unclear due to the existence of two different chairs which would present one group in an axial position, and the other in an equatorial position.

^{1}H-NMR spectroscopy was used to discern this equilibrium (Fig. 6). Several spectra were recorded in three solvents, *i.e.* $CDCl_3$, CD_3CN, and acetone-d_6, the latter two were used as reaction solvents in the enzymatic resolution of (±)-**4**.[7] Spectra at 30 °C and at low temperature were also obtained to study the main conformation. The peak of H-1 (H α to the ester) was used in the analysis since it is well resolved as a ddd without any overlapping at 2.4–2.5 ppm. In all the spectra, no signal splitting was observed at low temperature, instead a similar pattern was always seen: one coupling constant of 11–12 Hz (typical $^3J_{HH}$ ax–ax), and two of 3–4 Hz (typical $^3J_{HH}$ ax–eq or $^3J_{HH}$ eq–eq). This unequivocally confirms H-1 in an axial position with a large ax–ax coupling constant with *trans*-H-6, and two small $^3J_{HH}$ ax–eq with H-2 and *cis*-H-6. Thus, in the major conformation of (±)-**4** the hydroxyl group lies in an axial position. Hence, this more stable conformer of *R*-**4** was investigated first (Fig. 7A).

The cyclohexane lies in the medium-sized pocket of the active site and the ester group in the large pocket with the oxygen of the carbonyl pointing out towards the solvent. In this structure,

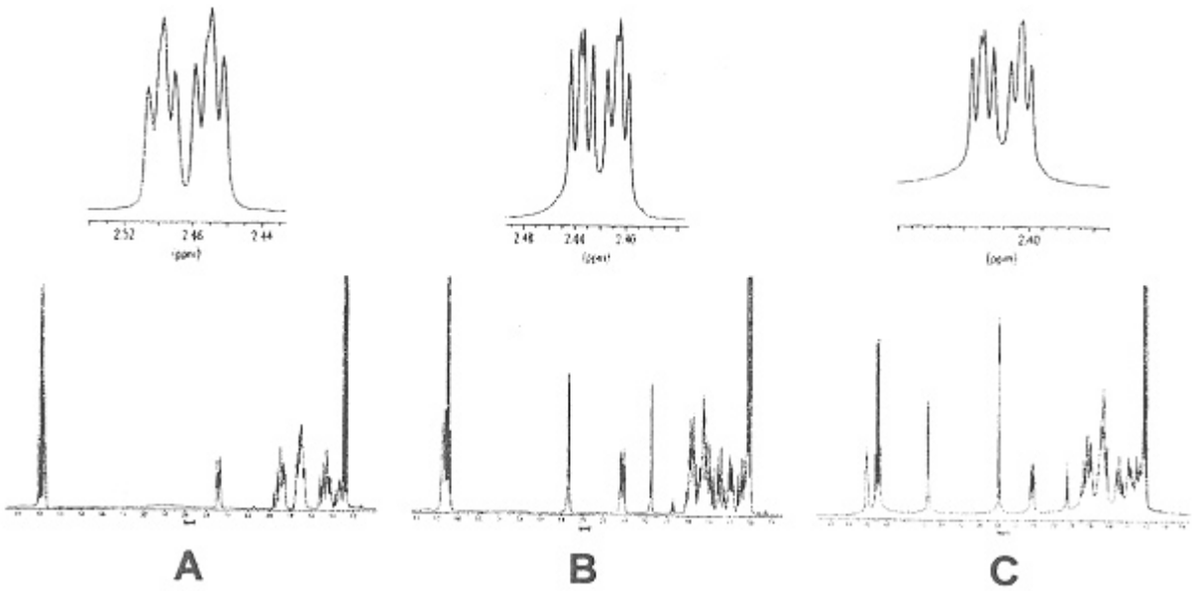

Fig. 6 ^{1}H-NMR spectra of compound (±)-**4** (below) and expanded signal of H-1 (above) in: A) $CDCl_3$; B) CD_3CN; and C) acetone-d_6.

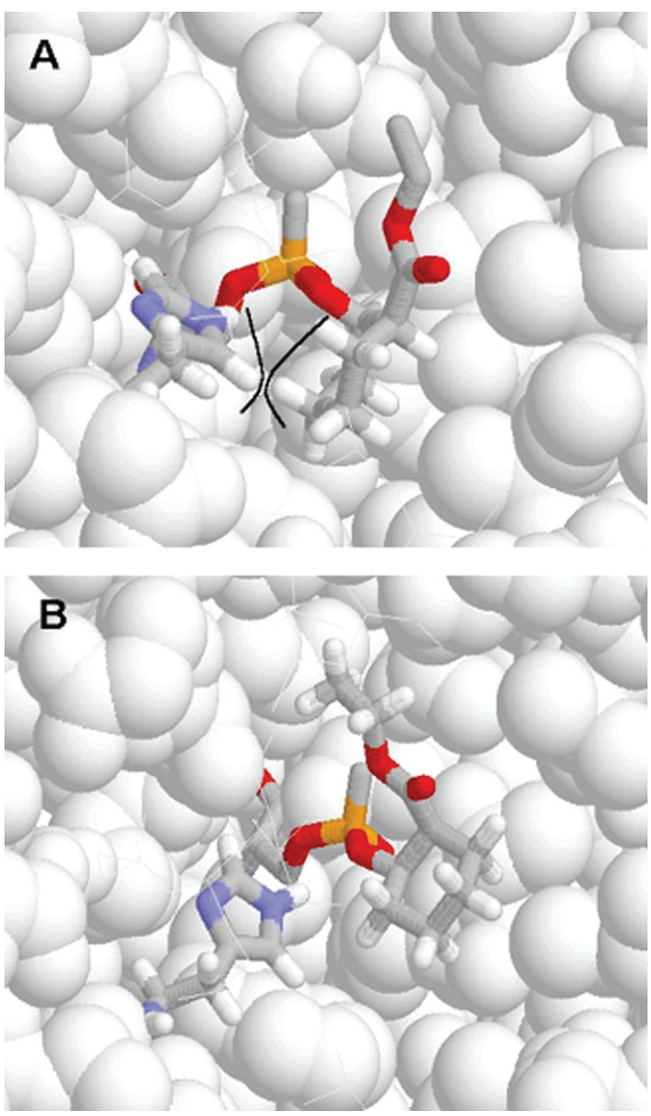

Fig. 7 Models for the *O*-acetylation of the *R* enantiomer of cyclohexanol **4** in two different conformations: A) OH in axial position; B) OH in equatorial position. Above images display some amino acids in a wireframe representation to allow a better view of the structure.

cis-hydrogen atoms in 3,5-diaxial positions with respect to the hydroxyl group clash with the catalytic histidine (Fig. 8B). These steric hindrances in the active site were enough to disrupt the necessary interaction with the nucleophile, and therefore, the energy of the intermediate is destabilised by 6.4 kcal.mol^{-1} in comparison with the *trans* isomer *R*-**2** (Row 3 in Table 2). These observations can explain the lower reactivity of the *cis*-*R*-isomer.

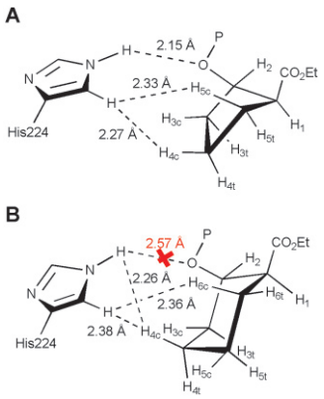

Fig. 8 Schematic showing the steric hindrance between His224 and: A) *R*-**3**; B) *R*-**4**. Hydrogen bond lost is marked with a red cross.

Subsequently, the phosphonate analogue with the hydroxyl group in an equatorial position was built and minimised (Fig. 7B). We obtained a structure in which all key hydrogen bonds are present, but the energy of the system is almost 3 kcal mol^{-1} higher than its conformer in Fig. 7A (Row 4 in Table 2). This fact could be due to two main factors: first, a higher-energy conformation of the cyclohexane, and secondly, a weaker binding of the substrate within the active site. The ring does not lie in the medium-sized pocket because of steric hindrance between His224 and the ester in the axial position, resulting in the loss of stabilising van der Waals interactions.

Lastly, the intermediate of *S*-**4** was minimised (Fig. S4 in ESI†). Although the best structure had a similar energy compared with the one obtained for the *R* enantiomer, some crucial hydrogen bonds were lost (Row 5 in Table 2), explaining the even lower reactivity of CAL-B towards this enantiomer.

3. Conclusions

Although the results of biotransformations are more predictable today than ten years ago, still some trends remain which cannot be explained satisfactorily; *e.g.* the lack of reactivity of *cis*-1,2-disubstituted cyclohexanols in lipase-catalysed acylation processes. Using computer-aided molecular modelling, a molecular basis for the acylation of different cyclic β-hydroxy esters has been proposed in this paper.

The *R*-enantiopreference for these compounds shown by CAL-B is in good agreement with Kazlauskas' rule.[23] The preferred enantiomers adopt a more favourable ring conformation, in which their binding into the active site is improved. In contrast, *S* enantiomers had a worse interaction with the catalytic triad, and crucial hydrogen bonds were lost in some cases.

Furthermore, we have explained the low reactivity of the *cis*-cyclohexanol derivative. In its major conformation with the hydroxyl group in an axial position, the *cis*-hydrogens in 3,5-diaxial positions impeded the reaction due to steric hindrance. However, the five-membered analogue can react due to the smaller size and the better ring conformation.

The results shown can also explain related experimental facts, such as the lack of reactivity of several *trans*-1,3-disubstituted cyclohexanes.[24] In this class, the group in the 3 position would be preferentially placed in an equatorial disposition while the hydroxyl group would be in an axial position. The model proposed by us is in accordance with the good reactivity of *cis*-2-cyanocyclohexanol with lipases,[3a] since small groups in the 2 position would favour a ring conformation with an equatorial hydroxyl group. This model can explain the reactivity of *cis*-1,2-cyclopentanols and of cycloheptanols. The seven-membered analogues could adopt several energetically similar conformers,[25] thus allowing for many different dispositions within the active site of the enzyme, and by this being able to react more easily, despite their bigger size.

4. Experimental section

4.1. General

Compounds (±)-**2**, (±)-**3** and (±)-**4** are commercially available from Aldrich and were used without further purification. Compound (±)-**1** was synthesised using a procedure similar to that reported by Nakata and Oishi.[7,26] ^{1}H-NMR spectra were obtained with a Bruker AMX 400 (400.13 MHz) spectrometer, using $CDCl_3$, CD_3CN and acetone-d_6 as solvents.

4.2. Computational details

The program Insight II, version 2000.1, was used for viewing the structures. The geometric optimisations were performed using Discover, version 2.9.7 (Accelrys, San Diego, CA, USA), using the AMBER force field.[14] The distance dependent dielectric constant was set to 4.0 and the 1–4 van der Waals interactions were scaled to 50%. The crystal structure of CAL-B (1LBS)[18] was obtained from the Protein Data Bank (www.rcsb.org/pdb/).

Hydrogen atoms were added to the structure, tested for partial charge balance and corrected for atom types within the AMBER force field. The pH of the catalytic histidine was adjusted to pH 4 and the structure was then relaxed. Geometry optimisations were carried out in two steps. First, the steepest descent algorithm got the molecule to a local minimum with a RMS deviation of about 0.02 Å mol^{-1}. Secondly, a conjugate gradient algorithm gave a more precise minimisation near the local minimum, obtaining an RMS value of 0.005 Å mol^{-1}.

Next, a phosphonate core of the tetrahedral intermediate mimicking methylation of methanol was assembled in the crystal structure. Partial charges on the intermediate atoms were set to those of the tetrahedral intermediate (carbon, not phosphorus), obtaining the values by semi-empirical calculation performed using Chem3D using the AM1 parameters.

For the optimisation of this phosphonate core a systematic approach was applied. Initially, the intermediate was allowed to adjust to the enzyme active site by keeping the entire enzyme fixed during the geometry optimisation. The side chains of the lipase were then released and allowed to adjust. Finally, the entire complex was allowed to adjust. This approach avoided drastic changes in the lipase structure caused by non-optimal conformations of the intermediate until an RMS maximum value of 0.005 Å mol^{-1} was obtained. A hydrogen bond calculation was performed after each minimisation in order to assure the presence of the critical hydrogen bonds around the catalytic site.[19]

The rest of the molecule was added and different conformations were produced by manual adjustment of dihedral angles specified in Fig. 9. Geometry optimisations were again performed using the same approach described above. Due to the flexible structure of these intermediates, small adjustments of the dihedral angle *a* caused large changes in the orientation of the ester moiety. Adjustments of approximately 10–20° were performed for both dihedral angles adjacent to that position. Structures causing obvious steric hindrance were ignored.

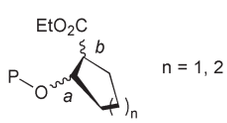

Fig. 9 Manipulated dihedral angles for the intermediates.

Acknowledgements

Financial support of this work by the Spanish Ministerio de Ciencia y Tecnología (Project No. PPQ-2001-2683) and by Principado de Asturias (Project No. GE-EXP01-03) is gratefully acknowledged. I.L. thanks MCYT for a pre-doctoral fellowship.

References

1 (*a*) C. J. Sih and S.-H. Wu, *Top. Stereochem.*, 1989, **19**, 63; (*b*) U. T. Bornscheuer and R. J. Kazlauskas, *Hydrolases in Organic Synthesis: Regio- and Stereoselective Biotransformations*, Wiley-VCH, Weinheim, 1999.

2 A. Liese, K. Seelbach and C. Wandrey, *Industrial Biotransformations*, Wiley-VCH, Weinheim, 2000.

3 (*a*) E. Forró, K. Lundell, F. Fülöp and L. T. Kanerva, *Tetrahedron: Asymmetry*, 1997, **8**, 3095; (*b*) A. Maestro, C. Astorga and V. Gotor, *Tetrahedron: Asymmetry*, 1997, **8**, 3153; (*c*) A. Luna, C. Astorga, F. Fülöp and V. Gotor, *Tetrahedron: Asymmetry*, 1998, **9**, 4483; (*d*) E. Forrö, Z. Szakonyi and F. Fülöp, *Tetrahedron: Asymmetry*, 1999, **10**, 4619; (*e*) L. M. Levy and V. Gotor, *J. Org. Chem.*, 2004, **69**, 2601.

4 J. González-Sabín, V. Gotor and F. Rebolledo, *Tetrahedron: Asymmetry*, 2004, **15**, 1335.

5 J. K. Whitesell, *Chem. Rev.*, 1992, **92**, 953.

6 (*a*) D. H. Apella, L. A. Christianson, D. A. Klein, D. R. Powell, X. Huang, J. Barchi, Jr. and S. H. Gellman, *Nature (London)*, 1997, **387**, 381; (*b*) A. Pecunioso, M. Maffeis, C. Marxhioro, L. Rossi and B. Tamburini, *Tetrahedron: Asymmetry*, 1997, **8**, 775; (*c*) E. Racanska and F. Gregan, *Pharmazie*, 1999, **54**, 68.

7 L. M. Levy, J. R. Dehli and V. Gotor, *Tetrahedron: Asymmetry*, 2003, **14**, 2053.

8 (*a*) E. Forró, L. T. Kanerva and F. Fülöp, *Tetrahedron: Asymmetry*, 1998, **9**, 513–520; (*b*) C. Brunet, M. Zarevucka, Z. Wimmer and M.-D. Legoy, *Enzyme Microb. Technol.*, 2002, **31**, 609.

9 E. Forró and F. Fülöp, *Tetrahedron: Asymmetry*, 1999, **10**, 1985.

10 R. Tanikaga, Y. Matsumoto, M. Sakaguchi, Y. Koyama and K. Ono, *Tetrahedron Lett.*, 2003, **44**, 6781.

11 E. L. Eliel and F. J. Biros, *J. Am. Chem. Soc.*, 1966, **88**, 3334.

12 D. J. Pasto and D. R. Rao, *J. Am. Chem. Soc.*, 1970, **92**, 5151.

13 (*a*) R. J. Kazlauskas, *Curr. Opin. Chem. Biol.*, 2000, **4**, 81; (*b*) R. Kazlauskas, *Science*, 2001, **293**, 2277.

14 (*a*) S. J. Weiner, P. A. Kollman, D. A. Case, U. C. Singh, C. Ghio, G. Alagona, S. Profeta and P. Weiner, *J. Am. Chem. Soc.*, 1984, **106**, 765; (*b*) W. D. Cornell, P. Cieplak, C. I. Bayly and P. A. Kollmann, *J. Am. Chem. Soc.*, 1993, **115**, 9620.

15 S. Park, E. Forró, H. Grewal, F. Fülöp and R. J. Kazlauskas, *Adv. Synth. Catal.*, 2003, **345**, 986.

16 (*a*) F. Hæffner and T. Norin, *Chem. Pharm. Bull.*, 1999, **47**, 591; (*b*) K. Hult and P. Berglund, *Curr. Opin. Biotechnol.*, 2003, **14**, 395.

17 C. S. Chen, Y. Fujimoto, G. Girdaukas and C. J. Sih, *J. Am. Chem. Soc.*, 1982, **104**, 7294.

18 J. Uppenberg, N. Öhrner, M. Norin, K. Hult, G. J. Kleywegt, S. Patkar, V. Waagen, T. Anthonsen and T. A. Jones, *Biochemistry*, 1995, **34**, 16838.

19 To identify hydrogen bonds, a donor atom to acceptor atom distance of less than 3.20 Å and a donor atom–hydrogen–acceptor atom angle of 120° or greater are required.

20 Several ^{1}H-NMR spectral data of (±)-**2** were recorded in different solvents, and signals of H-1 (α to the ester) and H-2 (α to the hydroxyl group), showed two $^3J_{HH}$ ax–ax (between 10–14 Hz) and one $^3J_{HH}$ between 3–5 Hz, typically ax–eq. This indicates that both hydrogens must be in axial positions.

21 The relation between the difference in the Gibbs energy of the transition states of the enantiomers and the enantiomeric ratio can be shown with the transition state theory to be $\Delta_{R-S}\Delta G^{\ddagger} = \Delta G_R^{\ddagger} - \Delta G_S^{\ddagger} = -RT\ln E$.

22 R. J. Abraham, R. Koniotou and F. Sancassan, *J. Chem. Soc., Perkin. Trans. 2*, 2002, 2025.

23 R. J. Kazlauskas, A. N. E. Weissfloch, A. T. Rappaport and L. A. Cuccia, *J. Org. Chem.*, 1991, **56**, 2656.

24 (*a*) R. Tanikaga and A. Morita, *Tetrahedron Lett.*, 1998, **39**, 635; (*b*) L. M. Levy, G. de Gonzalo and V. Gotor, *Tetrahedron: Asymmetry*, 2004, **15**, 2051.

25 (*a*) D. F. Bocian and H. L. Strauss, *J. Am. Chem. Soc.*, 1977, **99**, 2876; (*b*) K. B. Wiberg, *J. Org. Chem.*, 2003, **68**, 9322.

26 T. Nakata and T. Oishi, *Tetrahedron Lett.*, 1980, **21**, 1641.